

ShakeOut Scenario Appendix B: Factors for Correcting Ground Motions at Large Distance from Empirical Models to be Compatible with Simulated Motions

By Lisa M. Star¹ and Jonathan P. Stewart¹

USGS Open File Report 2008-1150, Appendix B
CGS Preliminary Report 25B

2008

U.S. Department of the Interior
U.S. Geological Survey

California Department of Conservation
California Geological Survey

¹ University of California, Los Angeles

U.S. Department of the Interior
DIRK KEMPTHORNE, Secretary

U.S. Geological Survey
Mark D. Myers, Director

State of California
ARNOLD SCHWARZENEGGER, Governor

The Resources Agency
MIKE CHRISMAN, Secretary for Resources

Department of Conservation
Bridgett Luther, Director

California Geological Survey
John G. Parrish, Ph.D., State Geologist

U.S. Geological Survey, Reston, Virginia 2008

For product and ordering information:
World Wide Web: <http://www.usgs.gov/pubprod>
Telephone: 1-888-ASK-USGS

For more information on the USGS—the Federal source for science about the Earth, its natural and living resources, natural hazards, and the environment: World Wide Web: <http://www.usgs.gov>
Telephone: 1-888-ASK-USGS

Suggested citation:

Star, L.M., and Stewart, J.P., 2008, ShakeOut Scenario Appendix B; Factors for correcting ground motions at large distance from empirical models to be compatible with simulated motions, Appendix B *of* Jones, L.M., and others, The ShakeOut Scenario: U.S. Geological Survey Open-File Report 2008-1150, and California Geological Survey Preliminary Report 25B, 8 p.
[http://pubs.usgs.gov/of/2008/1150/appendixes/of2008-1150_appendix_b.pdf].

Any use of trade, product, or firm names is for descriptive purposes only and does not imply endorsement by the U.S. Government.

Although this report is in the public domain, permission must be secured from the individual copyright owners to reproduce any copyrighted material contained within this report.

SHAKEOUT: Factors for Correcting Ground Motions at Large Distance from Empirical Models to be Compatible with Simulated Motions

By Lisa M. Star and Jonathan P. Stewart
University of California, Los Angeles

The ground motions being used to represent the effects of a large San Andreas fault earthquake for use in the ShakeOut Project are computed from a hybrid simulation procedure described in Graves (1996). In a parallel effort, we have been examining the consistency of the simulation results with empirical ground motion prediction equations (GMPEs). The principal findings of that work to date are described in Graves et al. (2008).

Portions of the study area being examined in the ShakeOut project do not have simulated motions. Those areas are generally to the east of the fault at a fault distance of 40 km and greater. Ground motions can be predicted for those portions of the study area from GMPEs, but because of general differences between the simulated and median empirical motions, this approach would produce a step in ground motions 40 km east of the fault. The purpose of this document is to develop factors to correct ground motions predicted from GMPEs so that they are consistent with the general character of the motions generated by the simulation procedure. These corrections will remove “steps” in the ground motions at the 40 km threshold distance. The GMPE used here is from Campbell and Bozorgnia (2007).

To develop correction factors, we begin by calculating residuals between the simulated and empirical motions as follows:

$$R_i(T) = \ln(S_a(T))_{sim,i} - \ln(S_a(T))_{GMPE,i} \quad (1)$$

where index i refers to an individual simulated ground motion at a particular latitude and longitude, $S_a(T)_{sim,i}$ refers to the spectral acceleration of the simulated motion for oscillator period T at location i , $S_a(T)_{GMPE,i}$ refers to the spectral acceleration for location i predicted by a GMPE, and R_i is the residual in natural logarithmic units.

Residuals from the simulations are compiled as a function of source distance r and parameters introduced by Somerville et al. (1997) to represent the effects of near-fault directivity for strike-slip earthquakes – X and θ . Parameters X and θ are defined in Figure 1, and are normally combined as $X \cos(\theta)$ to form a single parameter for rupture directivity.

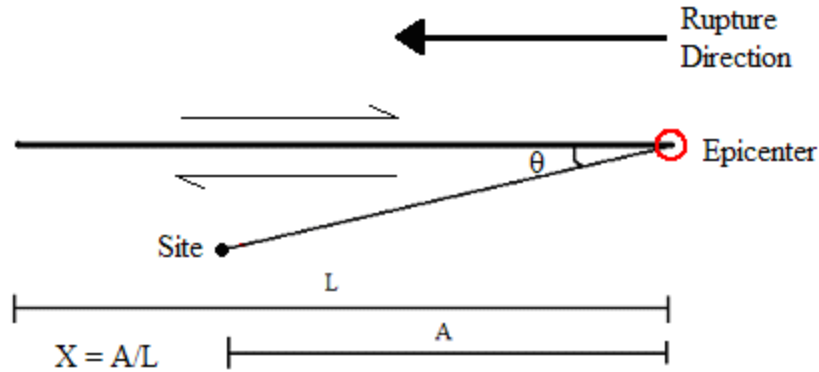


Figure 1. Schematic illustration of directivity parameters X and θ (adapted from Somerville et al., 1997)

The residuals for peak ground acceleration (PGA) are plotted as a function of distance (r) for various categories of $X \cos(\theta)$ in Figure 2. Figure 2a plots residuals for relatively low values of $X \cos(\theta)$, corresponding nearly to a backward directivity region. Figures 2b-d plot residuals for sites with progressively increasing directivity. Because the residuals in Figure 2 are qualitatively similar, the rupture directivity effect appears to be modest for PGA. Figure 3 shows the same results for $T=5$ sec spectral acceleration. The residuals for different bins of $X \cos(\theta)$ are somewhat more distinct from each other at longer periods. The median of the residuals in Figure 3a is generally lower as compared to the plots corresponding to larger $X \cos(\theta)$. Aside from the directivity effect, the distance effect is clear in each frame. The residuals show a significant negative trend at long distances (indicating simulated motions are less than the empirical median). This is generally true across the spectral periods examined.

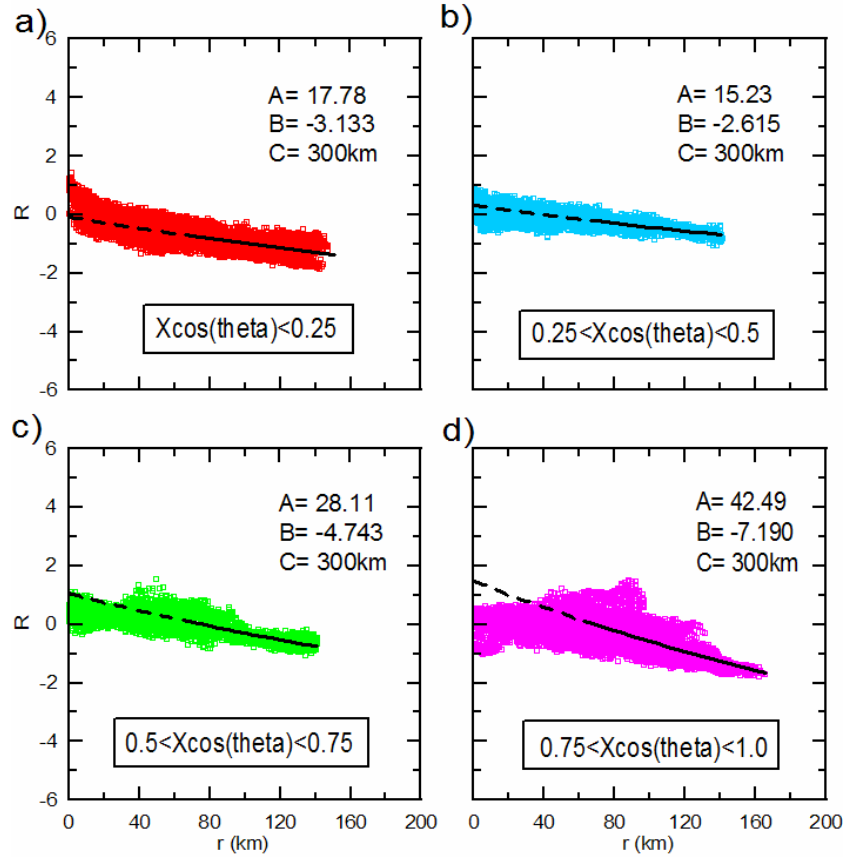


Figure 2. Residuals for PGA as a function of r , with regression fits and coefficients for a) $X\cos(\theta) < 0.25$, b) $0.25 < X\cos(\theta) < 0.5$, c) $0.5 < X\cos(\theta) < 0.75$, d) $0.75 < X\cos(\theta) < 1.0$. The regression fit is shown as solid in the range used for the regression ($r=70 - 165$ km). The dotted line is an extrapolation to $r=0$, showing the lack of fit in this range.

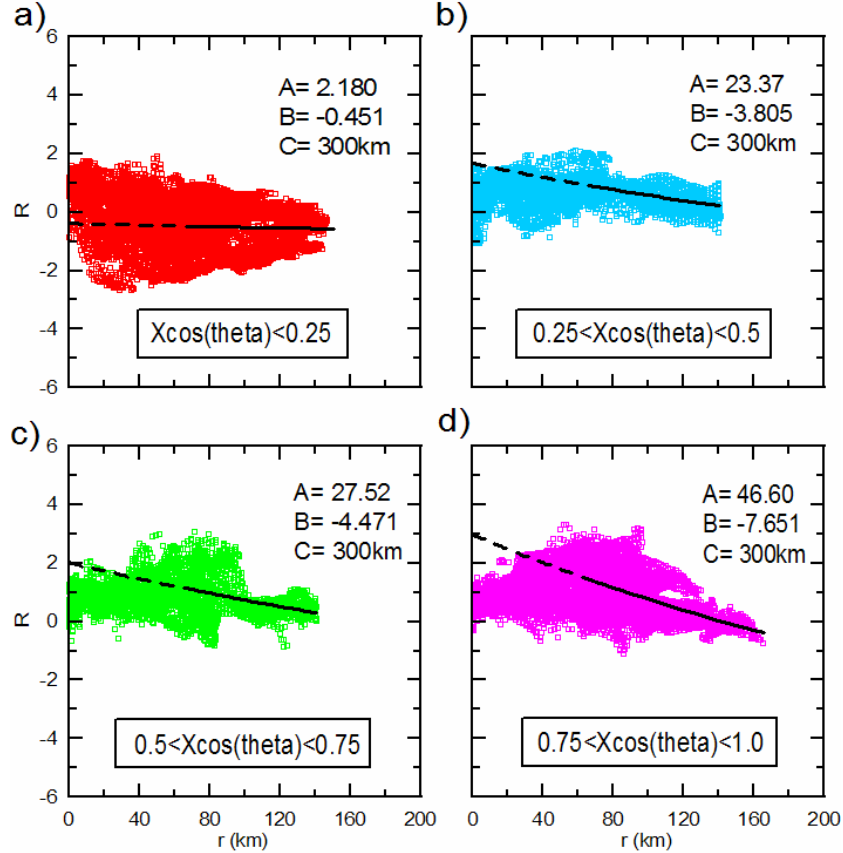


Figure 3. Residuals for 5.0 s period as a function of r , with regression fits and coefficients for a) $X\cos(\theta) < 0.25$, b) $0.25 < X\cos(\theta) < 0.5$, c) $0.5 < X\cos(\theta) < 0.75$, d) $0.75 < X\cos(\theta) < 1.0$. The regression fit is shown as solid in the range used for the regression ($r=70 - 165\text{km}$). The dotted line is an extrapolation to $r=0$, showing the lack of fit in this range.

To develop the correction factors, we perform regression analysis to relate residuals to r for each bin of $X\cos(\theta)$ shown in Figures 2-3. The regressions are performed according to the following equation:

$$R_i = A + B \times \ln(r_i + C) + \varepsilon_i \quad (2)$$

where A , B , and C are regression coefficients and ε_i is the residual of the regression for point i . Values of the regression coefficients for PGA and $T=5$ sec spectral acceleration are given in Figures 2 and 3, respectively. Values for other ground motion parameters are given in Table 1. Because the intended application is at large distance the regression is performed over the distance range of $r=70$ to 165 km. Note that C is held constant in the regressions at 300 km. There is some misfit at small distance that is not of concern for the present application.

We then performed regression analysis to relate coefficient A to $X \cos(\theta)$. The following equation was used for this analysis:

$$A_j = A_1 + A_2 \cdot X \cos(\theta) + A_3 \cdot (X \cos(\theta))^2 + \varepsilon_j \quad (3)$$

Index j refers to period (the regression is performed across values of A_j for different periods). Parameters A_1 - A_3 are regression coefficients and ε_j is the residual of the fit for the period corresponding to index j . Values for these parameters are given in Table 2.

A similar analysis was performed to relate the coefficient B to $X \cos(\theta)$. The regression was performed using the functional form:

$$B_j = B_1 + B_2 \cdot X \cos(\theta) + B_3 \cdot (X \cos(\theta))^2 + \varepsilon_j \quad (4)$$

The values of the coefficients B_1 , B_2 , and B_3 for various periods are also given in Table 2. Figure 4 shows the coefficients A and B determined on a period-by-period basis and the fit achieved with Eqs. 3-4.

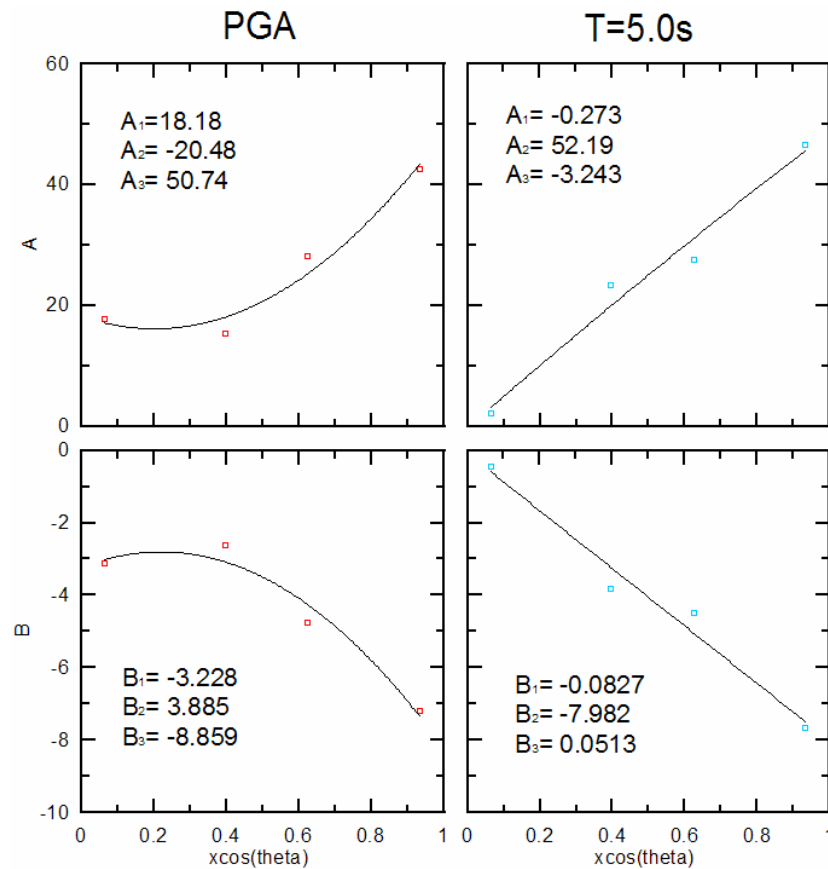


Figure 4. Coefficients A and B versus $X \cos(\theta)$ with fits lines for PGA and T=5.0s spectral acceleration.

By combining the Eq. 2 with Eqs. 3-4, mean residual R_m can then be related to r and $X \cos(\theta)$:

$$R_m = A_1 + A_2 \cdot X \cos(\theta) + A_3 \cdot (X \cos(\theta))^2 + \left[B_1 + B_2 \cdot X \cos(\theta) + B_3 \cdot (X \cos(\theta))^2 \right] \times \ln(r + C) \quad (5)$$

The corrected value of the ground motions for use in ShakeOut [$S_a(T)_{cor,i}$] can then be calculated by re-arranging Eq. 1 as:

$$\ln(S_a(T))_{cor,i} = R_m(T, r_i, X_i \cos \theta_i) + \ln(S_a(T))_{GMPE,i} \quad (6)$$

Where R_m is calculated from Eq. 5 using the site source distance (r) and $X \cos(\theta)$ specific to location i and $S_a(T)_{GMPE,i}$ is the predicted median spectral acceleration from a GMPE for location i . Figure 5 plots correction factor R for a range of periods as determined by Eq. 5.

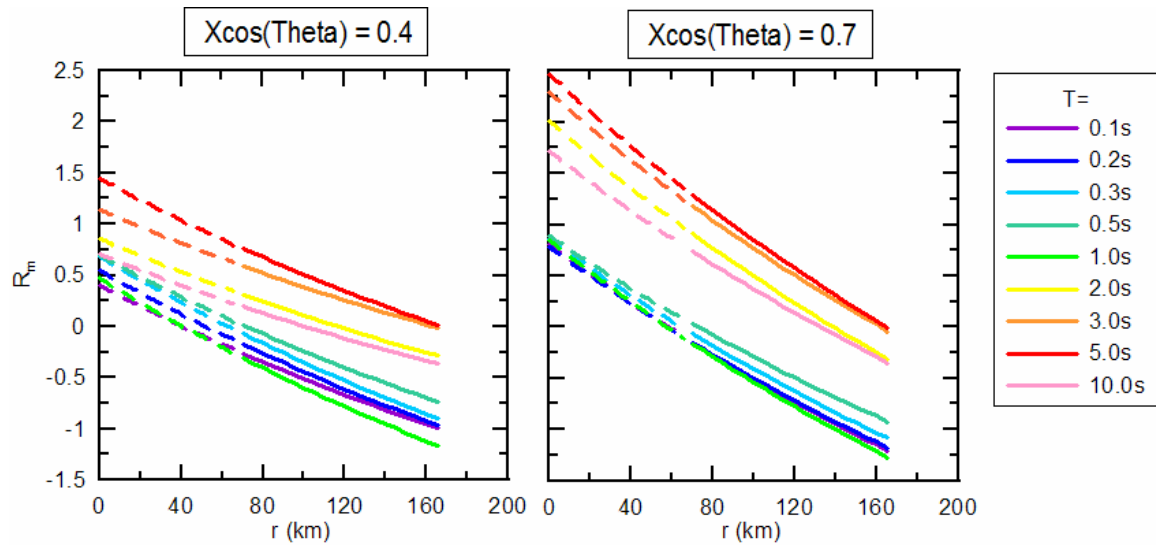


Figure 5. Correction factor R versus r for $X \cos(\theta) = 0.4$ and 0.7 for a range of periods.

Table 1. Values of regression coefficients for bins of $X \cos(\theta)$.

T (s)	Xcos θ	A	B	C (km)
0.1	<0.25	19.08	-3.359	300
	0.25-0.5	15.85	-2.739	300
	0.5-0.75	26.92	-4.565	300
	>0.75	38.11	-6.500	300
0.2	<0.25	20.16	-3.516	300
	0.25-0.5	18.69	-3.203	300
	0.5-0.75	25.89	-4.384	300
	>0.75	34.35	-5.880	300
0.3	<0.25	20.59	-3.567	300
	0.25-0.5	20.59	-3.503	300
	0.5-0.75	25.28	-4.269	300
	>0.75	32.57	-5.564	300
0.5	<0.25	17.79	-3.082	300
	0.25-0.5	19.05	-3.225	300
	0.5-0.75	23.02	-3.879	300
	>0.75	30.81	-5.249	300
1	<0.25	16.96	-2.971	300
	0.25-0.5	25.42	-4.336	300
	0.5-0.75	22.71	-3.888	300
	>0.75	36.88	-6.253	300
2	<0.25	-0.828	-0.056	300
	0.25-0.5	19.142	-3.142	300
	0.5-0.75	24.31	-4.017	300
	>0.75	47.60	-7.878	300
3	<0.25	0.194	-0.156	300
	0.25-0.5	24.86	-4.057	300
	0.5-0.75	19.00	-3.080	300
	>0.75	50.58	-8.319	300
5	<0.25	2.180	-0.451	300
	0.25-0.5	23.368	-3.805	300
	0.5-0.75	27.52	-4.471	300
	>0.75	46.60	-7.651	300
10	<0.25	-8.825	1.364	300
	0.25-0.5	19.444	-3.232	300
	0.5-0.75	20.63	-3.400	300
	>0.75	36.67	-6.026	300
PGA	<0.25	17.78	-3.133	300
	0.25-0.5	15.23	-2.615	300
	0.5-0.75	28.11	-4.743	300
	>0.75	42.49	-7.190	300
PGV	<0.25	3.842	-0.791	300
	0.25-0.5	18.88	-3.134	300

	0.5-0.75	31.45	-5.206	300
	>0.75	48.60	-8.060	300

Table 2. Values of regression coefficients relating A and B to $X \cos(\theta)$.

T (s)	A1	A2	A3	B1	B2	B3
0.1	19.48	-19.49	43.13	-3.454	3.713	-7.615
0.2	20.44	-12.38	29.71	-3.592	2.504	-5.386
0.3	20.82	-7.600	21.83	-3.633	1.679	-4.048
0.5	17.95	-4.507	19.65	-3.133	1.150	-3.668
1.0	17.59	3.673	16.99	-3.085	-0.437	-2.967
2.0	-2.616	41.03	12.52	0.198	-5.962	-2.700
3.0	0.361	30.88	21.65	-0.224	-4.379	-4.125
5.0	-0.273	52.19	-3.243	-0.0827	-7.982	0.0513
10.0	-12.68	81.49	-32.27	1.983	-13.19	5.197
PGA	18.18	-20.48	50.74	-3.228	3.885	-8.859
PGV	1.028	42.05	9.645	-0.359	-6.362	-2.043